Invited paper at the 21st INS International Symposium on Rapidly Rotating Nuclei 1992, Tokyo, October 26-30, 1992

The submitted manuscript has been author by a contractor of the U. S. Governme under contract No. W-31-109-ENG-3 Accordingly, the U. S. Government retains nonexclusive, royalty-free license to publi or reproduce the published form of th contribution, or allow others to do so, fo U. S. Government purposes.

SOME 9210349--6

ANL/PHY/CP--78720

DE93 007899

Feeding and Decay of Superdeformed States

T. L. Khoo, T. Lauritsen, I. Ahmad, M. P. Carpenter, P. B. Fernandez, R. V. F. Janssens, E. F. Moore, F. L. H. Wolfs
Physics Div., Argonne National Lab., 9700 S. Cass Ave., Argonne, IL 60439

Ph. Benet, P. J. Daly
Purdue University, West Lafayette, IN 47907

K. B. Beard, U. Garg, D. Ye
University of Notre Dame, Notre Dame, IN 46556

M. W. Drigert
Idaho National Engineering Lab., Idaho Falls, ID 83415

RECEIVED
FEB 18 1993
OSTI

Abstract

The mechanisms for feeding and decay of superdeformed (SD) bands are examined. Data connected with both processes in ^{192}Hg are compared with model calculations. The calculations successfully reproduce the data, suggesting that the mechanisms for both processes are understood. Constraints on the energy of the SD band energies and on the well-depths at low and high spins have been obtained. At the point of decay around spin 10, we suggest that the SD band is 3.3-4.3 MeV above the normal yrast line and that the well depths at spin 10 and 40 are 0.5-1.3 and 3.5-4.5 MeV, respectively.

I. Introduction

The occurrence of a superdeformed (SD) secondary minimum in the potential energy surface is a direct consequence of shell structure [1]. Knowledge of the properties of the pocket, thus, provides first-hand knowledge of the shell correction. It is important to know, for example,

MASTER

DISTRIBUTION OF THIS DOCUMENT IS UNLIMITED

the energy of the SD minimum with respect to that of normal states with smaller deformation. What is the depth of the SD pocket and how does it change with spin? Experiment has so far provided little direct information despite the observation of over 50 SD bands in the A = 150 and 190 regions. Discrete line spectroscopy has provided information on the moments of inertia and microscopic configurations of the ground and low-lying states in the SD well, as well as on the pair correlations present in these elongated, rapidly-rotating states (see e.g. Ref. 2 for a review). The excitation energy of the SD states is, in general, not known (although it has recently been determined [3] in ^{143}Eu). Furthermore, the barrier penetration process has not been extensively studied to deduce the height and thickness of the barrier separating SD and normal states, or the inertial masses and the role of pairing associated with the tunneling motion. These topics will be discussed in this talk and in the following two by Shimizu and Sletten, in a session devoted to these subjects. Calculations on the feeding process have been performed by Schiffer and Herskind [4] and on the decay by Vigezzi et al. [5].

Properties of the fission barrier have been deduced from studies of fission isomers [1], and there certainly was a lot of excitement in the heydays of fission isomers! We are recapturing some of the same thrill in our studies of superdeformation today.

A secondary excited minimum is commonly referred to as a false vacuum in other fields of physics. Thus, study of SD states provides us a marvelous opportunity to study physics in a false vacuum.

A common element in the feeding and decay processes is the mixing between SD and normal sates. The mixing, in turn, is governed by the level density ρ of the respective states and the coupling (through tunneling) between them. Thus, by studying both processes we can infer information on ρ and the coupling, and thereby, obtain constraints on the excitation energy of SD states and the depth of the SD well.

II. Feeding of Superdeformed States

The observables through which we can study the feeding of SD bands include: (i) the intensities of the SD bands relative to the ground state population, (ii) the change of the SD intensities with spin, (iii) entry distributions (iv) quasicontinuum spectra of γ rays preceding the SD band

transitions, (v) the lifetimes and feeding times of SD band levels, and (vi) E_γ-E_γ correlation matrices. We shall discuss here mainly the first three items, although the other items have been used in our analysis but will only be touched upon here.

In this talk, we shall consider only data for normal and SD states of ^{192}Hg. (The physics conclusions, of course, apply to all SD states.) The ^{160}Gd (^{36}S,4n) reaction was employed, using beams (with a mid-target energy of 159 MeV) from ATLAS. γ rays were detected in the Argonne-Notre Dame γ-ray facility. Discrete lines were detected in 12 Compton-suppressed spectrometers (CSG), and fold K and sum-energy H were measured in a 50-element BGO hexagonal array. Gates were set on selected pairs of coincident lines in the CSGs to generate two-dimensional (K,H) matrices associated with feeding of either all (mostly normal) or SD states in ^{192}Hg. The entry distributions were obtained after correcting for the instrumental response and conversion of K to multiplicity and of multiplicity to spin I. The procedure is briefly described in Ref. 6. The entry distribution (I,E) represents the 2-dimensional population distribution in spin I and excitation energy E, from which γ decay starts after particle evaporation.

The entry distributions for all states in ^{192}Hg and for the SD states are shown in Fig. 1(a) and (b). Also shown in these figures are lines denoting the normal yrast states (extrapolated beyond spin 30), the SD yrast band, and the top of the barrier separating normal and SD states. The SD state is seen to originate from the portion of the total channel entry distribution which lies at high angular momentum. A superposition of Fig. 1(a) and (b) reveals that the entry distribution for SD states has slightly lower energy at a given spin than that for all states.

To understand how the compound nucleus decays and becomes trapped in the SD minimum, we have developed a Monte Carlo model to follow the γ decay process. Two classes of states are considered in the model: SD and normal states (the latter are defined as all non-SD states). The calculation starts with the <u>measured</u> entry distribution for all states in a given nucleus, with equilibrium assumed between the two classes of states. In other words, the prior history of particle decay is not considered relevant for the population of SD states, an assumption which is borne out by the results of the model (see below).

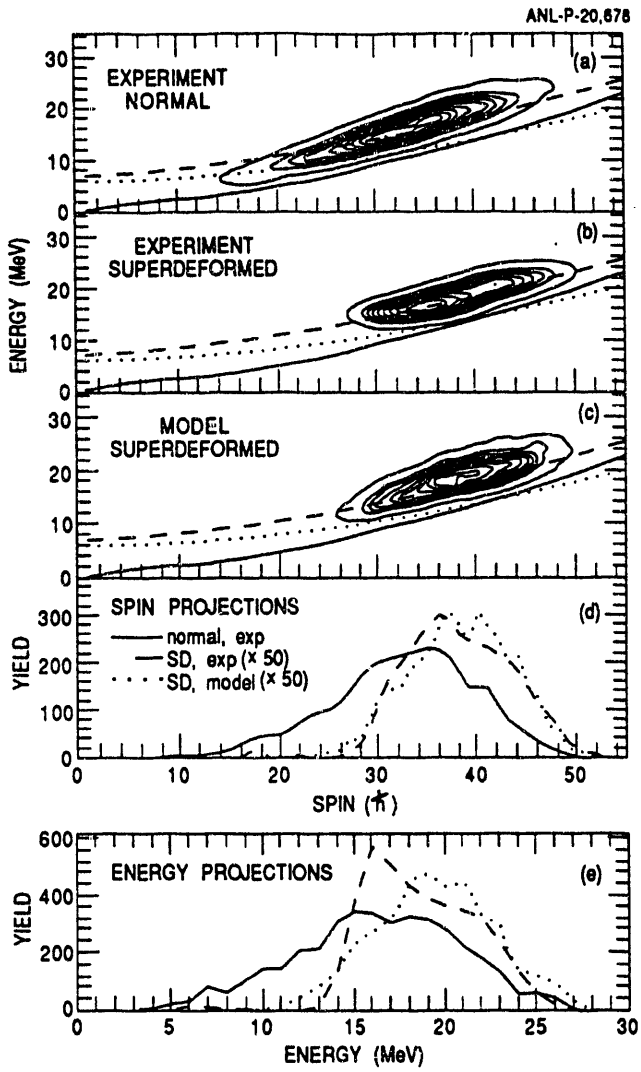

Fig. 1. Measured entry distributions leading to the population of (a) normal and (b) SD states in ^{192}Hg; contours represent changes of 10% of the maximum value. (c) Calculated entry distribution for SD states. (d) and (e) show the projections on the spin and energy axes, respectively, for the measured and calculated entry distributions; the SD distributions are multiplied by 50. Also shown in Fig. a-c are the normal (solid line) and SD (dots) yrast lines, and the barrier separating the two classes of states (dash). The SD band and barrier shown here give the best overall agreement between calculation and experiment.

At each step of the decay, either a collective stretched E2 or a statistical E1 transition is possible, with probability determined by the respective transition rate. In the course of a transition, the shape of the nucleus can remain the same or it can change (SD to normal, or vice versa), as a consequence of admixtures between the two classes of states. The E2 γ-width is controlled by the transition quadrupole moment Q_t and moment of inertia $\mathcal{J}$ (which determines the γ energy) appropriate for each well. The statistical E1 width is governed by the level density parameter, a, in the usual Fermi gas formula and the γ strength function S_γ in each well. The parameters which characterize the properties of the nucleus and which affect the feeding process are given in Table I. Each parameter has a strong affect on one (or at most two) observables, which is indicated in the Table. Conversely, the observables constrain the parameters and reveal properties of the nucleus.

The energies of the SD band E_{SD}^{I} and the well-depth W_I (at spin I) are two parameters that we are particularly interested in. The excitation energies of the SD band levels are fixed by a single parameter, E_{SD}, the energy at I = 0; other levels are given by the measured transition energies E_γ [7] or, below I = 10, by E_γ obtained from extrapolation. E_{SD} has a strong affect on the intensity of the SD band (measured relative to the ground state population); a lower energy results in larger calculated intensity, as might be expected. Fig. 2 shows the calculated SD intensity as a function of E_{SD} for several values of the well depth W_{40} at spin 40. Notice that the measured [7] relative intensity of 2 ± 0.2% is only obtained for a small range of E_{SD} values between 5.75 and 6.25 MeV. However, a minor dependency on other parameters and the requirement of simultaneously reproducing <u>all</u> observables - which is the procedure we adopt - lead to larger range of acceptable values. Good fits to all available observables [items (i)-(v) above] lead to E_{SD} = 5.6-6.2 MeV and W_{40} = 3.5-4.5 MeV. Values in this range give $\chi^2 \leq 2\chi^2_{min}$ in a least squares fit of (a) the SD band intensity, (b) the feeding spin of the SD band, (c) the entry spin, (d) the width of the spin distribution, (e) the entry energy, (f) the width of the energy distribution, (g) and the energy of the quasicontinuum E2 peak. The upper bound on E_{SD} is given by the measured entry distribution (without any recourse to comparison with calculation) from the requirement that the SD band must lie below its entire entry distribution.

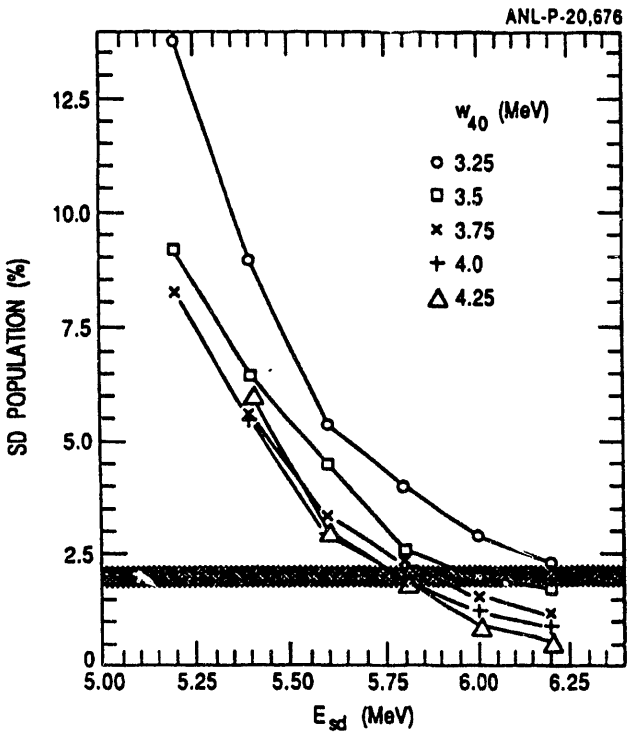

Fig. 2. Calculated intensity of the SD band (as a percentage of ^{192}Hg yield) as a function of SD energy E^0_{sd} for different values of SD well depth W_{40}. The measured[3] intensity of 2 ± 0.2% (shown in the shaded area) is obtained for only a narrow range of E^0_{sd}.

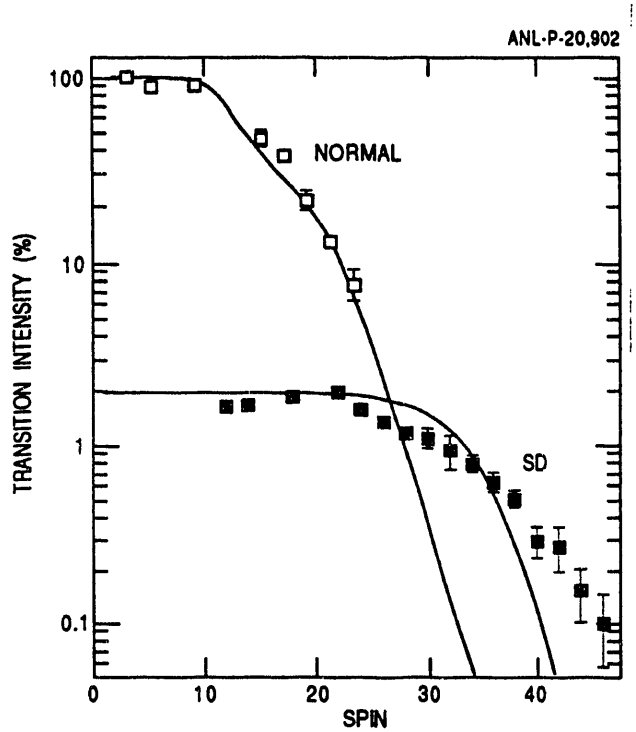

Fig. 3. Intensities of normal and SD yrast states in ^{192}Hg. Solid lines give calculated intensities; points are from experiment.

Table 1. Model Parameters and the Observables They Mainly Influence

Model Parameter[a]	Description	Value	Main Influence[b]
E_{sd}	SD at I=0 energy	5.4-6.2 MeV	Intensity
$W, \hbar\omega$	Barrier parameter	3.5-4.5,0.6 MeV	Entry distribution, $\langle E2_{sd}\gamma\rangle$
$\mathcal{J}_{sd}, \mathcal{J}_n$	Moment of inertia	121,61[c] $\hbar^2$ MeV^{-1}	$\langle E2_{sd}\gamma\rangle, \langle E2_n\gamma\rangle$
Q_{sd}, Q_n	Transition quadrupole moment	20,4[c] eb	Doppler shift of edge of quasi-continuum E2 spectrum
a_{sd}, a_n	Level density parameter	A/(8-14),A/8	Statistical spectra
Γ_{rot}	Rotational damping width	200 MeV	Ridge intensity in E_γ-E_γ matrix
U_0	Energy above yrast line for stopping cascade	~1.2 MeV	Feeding spin of SD band

[a]Subscripts "sd" and "n" refer to superdeformed and normal.

[b]Parameters have the strongest effect on these observables and smaller effects on other observables.

[c]Q_{sd} from SD band (Ref. 9); Q_n from Doppler shift of quasicontinuum spectrum feeding normal states.

Figure 1(c) shows that the calculation successfully reproduces the measured entry distribution leading to SD states. Naturally, the projections of the entry distribution on both the spin and energy axes are also reproduced - see Fig. 1 (d and e). Good agreement is also found for the intensities as a function of spin for both the SD band and the normal yrast states in ^{192}Hg - see Fig. 3.

The well-depth at spin 40, W_{40}, is quoted above since its value around this spin has a strong influence on the entry distribution. Theoretically, W_I is expected to increase with spin. To allow for this, we assume W_I increases with spin, fix W_0 at 1 MeV (the value calculated in Ref. 8), and vary W_{40}. Tunneling across the barrier also depends on the barrier width, characterized by the barrier frequency $\hbar\omega_B$, which we fix at 0.6 MeV, a somewhat arbitrary value adopted from Ref. 5-see section III.

Since the model is able to reproduce all known observables, we may employ it to give insight into the feeding mechanism of SD bands. Initially, for the hot nucleus, there is complete mixing between the SD and normal states. Consequently, there are jumps between the two classes of states, with an average of 2.2 jumps in each cascade. It is only when the cascade approaches the barrier that the probability for trapping in the SD well becomes significant. The trapping probability increases as the cascade approaches the minimum of the SD well and becomes very small when a discrete line SD band is finally fed. (However, the SD band does eventually jump to the normal states - see section III.) On average, trapping occurs around 1-2 MeV below the barrier. This may be seen in Fig. 4, which shows a sample of cascades which successfully populate SD band, i.e. are trapped in the SD pocket. Thin lines, which denote E2 transitions emitted by a nucleus with SD shape, are seen to dominate 1-2 MeV below the barrier. Thus, the decision on trapping occurs rather late, $\sim 10^{-14}$ s after formation of the compound nucleus, well after the time for particle emission and shape relaxation. This justifies our use of the measured entry distribution as the starting stage of the γ cascade.

The feeding mechanism revealed by the model provides an explanation for a number of phenomena. The E2 transitions in Fig. 4 lead to pronounced E2 peak centered around 0.7 MeV and to ridges in a E_γ-E_γ matrix. We have observed both features in our data. The model also shows

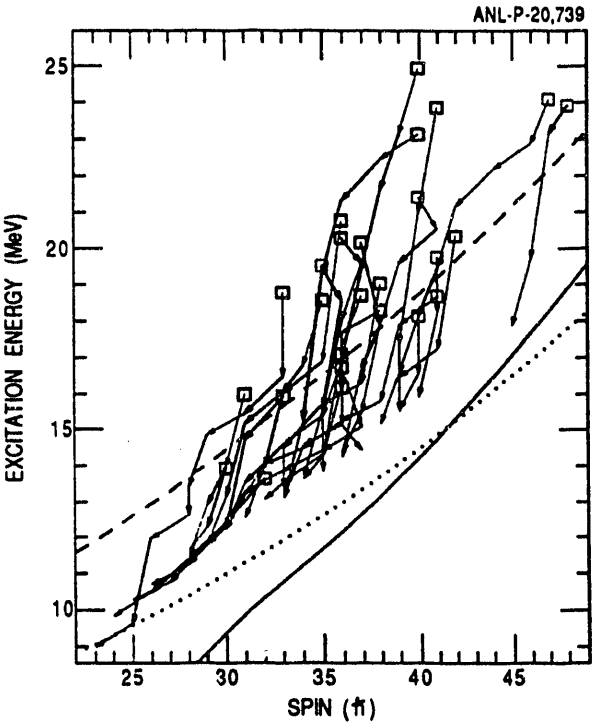

Fig. 4. Sample of 25 cascades which populate SD bands. Transitions are denoted by thick lines when the initial shape is normal and by thin lines when it is SD. Thick or thin squares indicate either normal or SD shapes, respectively, at the starting point of a cascade. See the caption of Fig. 1 for a description of solid, dotted and dashed lines.

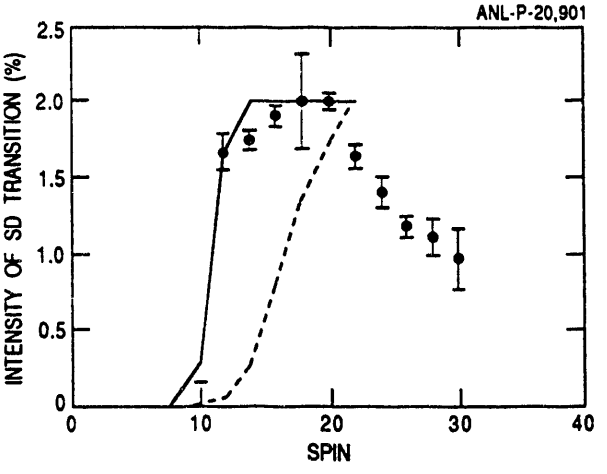

Fig. 5. Intensities of SD transitions (as a percentage of the total ^{192}Hg population) vs. spin. Lines are average intensities from calculations performed with a well depth which varies with spin (solid) or which remains constant (dash).

that cascades with E2 transitions below the barrier in the SD well can still escape out of the well. This should lead to higher intensities in the E_γ-E_γ ridges than for SD bands - as observed. The model also explains why SD bands are fed with larger intensity when the entry distribution of the nucleus of interest is cold. For higher initial E*, the cascade will reach the discrete SD band at lower spin due to the competition between cooling statistical transitions and non-cooling E2 transitions. At lower spin, W is smaller and the SD band is higher above the normal yrast line, leading to a lower value for ρ_{SD}/ρ_n; both disfavor the population of SD states.

III. Decay of Superdeformed Bands

The observables for studying the decay of SD bands are: (i) the variation of SD intensity with spin, (ii) the spin distribution of normal yrast states following the decay, (iii) the spectrum of the decay γ rays, (iv) peaks in spectra obtained by summing two (or more) decay lines - see talk by Sletten and Ref. 3, and (v) lifetimes. We concentrate here only on item (i).

When the γ cascade reaches the ground or low-lying states in the SD well, sharp intraband E2 transitions are emitted from levels which are isolated from the normal states. This isolation leads to an impressively long series of about 20 equally-spaced transitions; however, the intensities of the lines drop suddenly - see Fig. 5. This sudden disappearance of SD lines is a general feature and occurs around spin 10 in the A = 190 region and around spin 25 in the A = 150 region. Another common feature is that the decay pathways through which the SD bands decay to the lower-lying normal states must be highly fragmented; this is deduced from the fact that no individual path has yet bee found. What is the cause for the sudden decay? Is it due to mixing with normal states or to a disappearance of the barrier? Can we obtain information on W_I and how it changes with spin from the decay process?

Following Vigezzi et al. [5], we suggest that the decay is attributed to mixing with normal states. As the spin decreases, the energy of the SD state above the yrast line grows, so that the SD level is embedded in a sea of normal states with increasing level density - see Fig. 6. Coupling between SD and normal states leads to a spreading of the SD state among the normal states, characterized by a spreading width Γ. Thus, although

ANL-P-20,904

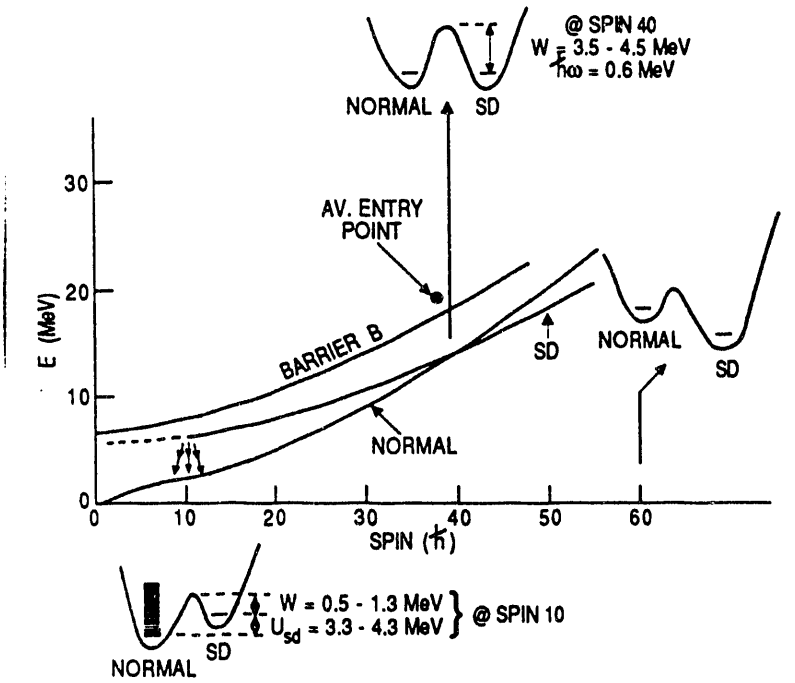

Fig. 6. Summary of some information on feeding and decay of SD states. Energies of normal and SD yrast lines in ^{192}Hg, and of the barrier separating normal and SD states. The SD band excitation energy shown here is deduced from the feeding process. Typical well depths at different spins are shown (but not to scale).

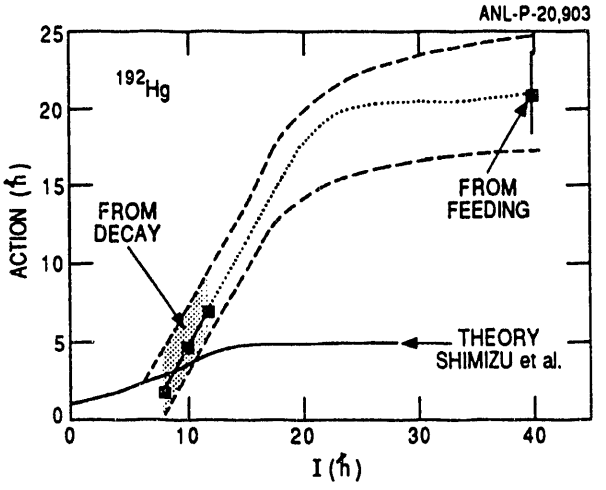

Fig. 7. Action associated with barrier penetration deduced from the feeding and decay of the SD band in ^{192}Hg. The envelope represents uncertainties due to possible variations of the level densities. Values calculated by Shimizu et al. [11] are also shown.

the coupling between SD and normal states is small (because of the barrier), mixing may occur when Γ/D_n acquires a finite value. D_n (= $1/\rho_n$) is the average spacing between normal states. In addition, with decreasing spin in the A = 190, the intraband E2 rate Γ_{SD} rapidly falls because of the growing fractional decrease in E_γ and the E_γ^5 dependence. Thus Γ_{SD}/Γ_n drops as spin decreases; Γ_n is the width for statistical decay for an excited normal state. This discussion emphasizes that the decay is governed by two quantities: Γ/D_n and Γ_{SD}/Γ_n. More details may be found in Shimizu et al. [11] and in Ref. [5].

We have performed calculations for ^{192}Hg based on the model proposed by Vigezzi et al. [5], who applied it for studying the decay of SD bands in the A = 150 region. Γ_{SD} is calculated using the transition quadrupole moment Q_t measured by Moore et al. [9], which was measured for states with I ~22-36. (Recent lifetime measurements by Lee et al. [10] for the lowest spin SD states in ^{192}Hg confirm that Q_t is the same around I = 10, where the decay occurs.) Γ_n is calculated using level densities given by a Fermi gas formula and a standard γ strength function. We have made calculations with the well depth W_{10} as a parameter which is adjusted to make the decay occur at the observed spin value. W is directly related to Γ:

$$W = -\frac{\hbar\omega_B}{2\pi} \ln \left\{\frac{2\pi}{\hbar\omega_s}\Gamma\right\} \qquad \text{Eq. 1}$$

Following Ref. 5, we have used $\hbar\omega_B = \hbar\omega_s = 0.6$ MeV. The calculated intensities (averaged to remove the stochasticity present in the decay process) are shown in Fig. 5. The solid line has been calculated using $W_{10} = 0.86$ MeV and $dW_I/dI = 0.25$ MeV/$\hbar$. To reproduce the sudden drop in SD intensity, <u>it is necessary to vary W_I with spin</u>. This was also found [5] to be necessary in the A = 150 region. If W_I is fixed at 0.86 MeV, the SD intensities drop gradually, as shown by the dashed line in Fig. 5.

The decay rate is dependent on Γ/D_n and, hence, on D_n. Since D_n is quite uncertain and could vary from 1/10 to 10 times the value given by the Fermi gas formula, there is a corresponding uncertainty in the deduced value of W_{10}. We are able to obtain a constraint, W_{10} = 0.5-1.3 MeV.

As shown in Eq. 1, the barrier tunnelling is governed not only by W, but also by $\hbar\omega_B$. Specifically it is the action, defined as $\pi W/\hbar\omega_B$ in the

inverse parabolic approximation, which characterizes the tunnelling. The action around spin 10 (from decay) and around spin 40 (from feeding) are shown on Fig. 7. For comparison, the theoretical action calculated by Shimizu et al. [11] is also shown. There is fair agreement at low spin, but the theoretical values at high spin are significantly lower than our inferred values. The origin of this discrepancy is not yet understood.

It is interesting to examine several of the quantities which affect the decay process. At the point of decay for ^{192}Hg $\Gamma/D_n \sim 3 \times 10^{-2}$, $\Gamma_{SD}/\Gamma_n \sim 5 \times 10^{-3}$, and the tunnelling probability is $\sim 1.5 \times 10^{-4}$. (Our analysis for ^{152}Dy gives corresponding values of approximately 12×10^{-2}, 0.6, and 7×10^{-4}.) Thus, the decaying SD state is still very sharp and is not spread among several normal states; in fact, it acquires a small component of only the nearest neighboring one or two normal states. The small values of Γ/D_n and of the tunnelling probability imply that the coupling between SD and normal states is extremely small, indicating that the barrier is still sizeable. Despite the small mixing which occurs between the two classes of states, the decay nonetheless happens because Γ_{SD} is much smaller than Γ_n.

As the SD band cascades down, an unusual phenomenon occurs: we have a sharp state, isolated in its own pocket, which is embedded in a sea of states with increasing level density. By proximity to a normal state, it inevitably acquires a small normal component at low spin, through which it decays to the lower-lying normal states. Since the relevant parameters should be similar for SD states in each of the A = 150 or 190 region, the spin at which the decay occurs should be similar in each mass region. Thus the model naturally explains why SD states decay around spin 10 in the whole A = 190 region and around spin 25 in the A = 150 region.

IV. Summary

The feeding and decay mechanisms of SD bands is now believed to be well understood. We have developed a model which can account for almost all of the observables connected with the feeding process and shows that trapping in the SD well occurs when the γ cascade reaches 1-2 MeV below the barrier. Model calculations of the decay process reproduce the decay of SD bands and partially attribute the suddenness of the decay to a decrease of W as spin decreases. By comparing data and the results of the

models, we constrain the energy of the SD band in ^{192}Hg to 3.3-4.3 MeV above the normal yrast line at the point of decay around spin 10. The well depths at spin 10 and 40 are 0.5-1.3 and 3.5-4.5 MeV, respectively, and implies that W_I changes with spin. A variation with spin is also necessary to reproduce the sudden decay out of the SD band into the normal states.

Acknowledgement

The code for Monte Carlo simulations of the feeding of SD bands built upon the code KLONK developed by R. Holzmann. We acknowledge helpful discussions with H. Esbensen, B. Herskind, W. Nazarewicz, K. Schiffer, Y.R. Shimizu, E. Vigezzi, and R. Wyss. This work was supported by the U.S. Department of Energy, Nuclear Physics Division, under contract W-31-109-ENG-38, No. DE-AC07-76ID01-570, and No. DE-FG02-87ER40346, and by the National Science Foundation under Grants No. PHY88-02279 and No. PHY91-00688.

REFERENCES

1 S. Bjørnholm and J.E. Lynn, Rev. Mod. Phys. 52 725 (1980).

2 R.V.F. Janssens and T.L. Khoo, Ann. Rev. Nucl. Part. Sci. 41 321 (1991).

3 A. Ataç, M. Piiparinen, B. Herskind, J. Nyberg, G. Sletten, G. de Angelis, S. Forbes, N. Gjørup, G. Hagemann, F. Ingebretsen, H. Jensen, D. Jerrestam, H. Kusakari, R. Lieder, G.M. Marti, S. Mullins, D. Santonocito, H. Schnare, K. Strahle, M. Sugawara, P.O. Tjøm, A. Virtanen and R. Wadsworth, Proc. Intenrnational Conference on Nuclear Structure at High Angular Momenta, Ottawa, 18-21 May, 1992 p. 42; Sletten et al., Proc. INS International Symposium on Rapidly Rotating Nuclei 1992, Tokyo, 26-30 October, 1992, this volume.

4 K. Schiffer, B. Herskind, and J. Gascon, Z. Phys. A 332 17 (1989); K. Schiffer and B. Herskind, Nucl. Phys. A520 521c (1990).

5 E. Vigezzi, R.A. Broglia and T. Døssing, Phys. Lett. B 249 163 (1990).

6 T. Lauritsen, Ph. Benet, T.L. Khoo, K.B. Beard, I. Ahmad, M.P. Carpenter, P.J. Daly, M.W. Drigert, U. Garg, P.B. Fernandez, R.V.F. Janssens, E.F. Moore, F.L.H. Wolfs, and D. Ye, Phys. Rev. Lett. 69 2479 (1992).

7 D. Ye et al., Phys. Rev. C 41 R13 (1990); J. Becker et al., *ibid.* 41 R9 (1990); T. Lauritsen et al., Phys. Lett. B 279 239 (1992).

8 W. Satuła, S. Ćwiok, W. Nazarewicz, R. Wyss and A. Johnson, Nucl. Phys. A529 289 (1991).

9 E.F. Moore, R.V.F. Janssens, I. Ahmad, M.P. Carpenter, P.B. Fernandez, T.L. Khoo, S.L. Ridley, F.L.H. Wolfs, D. Ye, K.B. Beard, U. Garg, M.W. Drigert, Ph. Benet, P.J. Daly, R. Wyss and W. Nazarewicz, Phys. Rev. Lett. 63 360 (1989).

10 I.Y. Lee, C. Baktash, D. Cullen, J.D. Garrett, N.R. Johnson, F.K. McGowan, D.F. Winchell, and C.H. Yu, Proc. Intenrnational Conference on Nuclear Structure at High Angular Momenta, Ottawa, 18-21 May, 1992 p. 21.

11 Y.R. Shimizu, et al., Proc. INS International Symposium on Rapidly Rotating Nuclei 1992, Tokyo, 26-30 October, 1992, this volume; Y.R. Shimizu, F. Barranco, R.A. Broglia, T. Døssing and E. Vigezzi, Phys. Lett. B274 243 (1992).

DISCLAIMER

This report was prepared as an account of work sponsored by an agency of the United States Government. Neither the United States Government nor any agency thereof, nor any of their employees, makes any warranty, express or implied, or assumes any legal liability or responsibility for the accuracy, completeness, or usefulness of any information, apparatus, product, or process disclosed, or represents that its use would not infringe privately owned rights. Reference herein to any specific commercial product, process, or service by trade name, trademark, manufacturer, or otherwise does not necessarily constitute or imply its endorsement, recommendation, or favoring by the United States Government or any agency thereof. The views and opinions of authors expressed herein do not necessarily state or reflect those of the United States Government or any agency thereof.

END

DATE
FILMED
4/7/93